

14 NBSIR-76-1115

6 Optical Materials Characterization.

10 Albert Feldman, Deane Horowitz and Roy M. Waxler

Marilyn J. Dodge

Inorganic Materials Division  
Institute for Materials Research

and

Marilyn J. Dodge

Optical Physics Division  
Institute for Basic Standards  
National Bureau of Standards  
Washington, D. C. 20234



11 August 1976

9 Semi-Annual Technical Report. 1 Feb - 31 Jul 76  
Period Covered: February 1, 1976 to July 31, 1976

15 ARPA Order No. 2620

16 NBS-313-0442

Prepared for  
Advanced Research Projects Agency  
Arlington, Virginia 22209

DISTRIBUTION STATEMENT A

Approved for public release;  
Distribution Unlimited

210800

NBSIR 76-1115

## OPTICAL MATERIALS CHARACTERIZATION

Albert Feldman, Deane Horowitz and Roy M. Waxler

Inorganic Materials Division  
Institute for Materials Research

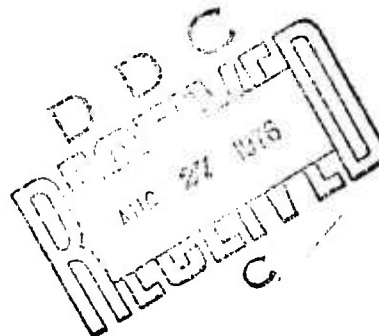
and

Marilyn J. Dodge

Optical Physics Division  
Institute for Basic Standards  
National Bureau of Standards  
Washington, D. C. 20234

August 1976

Semi-Annual Technical Report  
Period Covered: February 1, 1976 to July 31, 1976  
ARPA Order No. 2620



Prepared for  
Advanced Research Projects Agency  
Arlington, Virginia 22209



---

**U.S. DEPARTMENT OF COMMERCE, Elliot L. Richardson, Secretary**

**Edward O. Vetter, Under Secretary**

**Dr. Betsy Ancker-Johnson, Assistant Secretary for Science and Technology**

**NATIONAL BUREAU OF STANDARDS, Ernest Ambler, Acting Director**

OPTICAL MATERIALS CHARACTERIZATION

Albert Feldman, Deane Horowitz and Roy M. Waxler

Inorganic Materials Division  
Institute for Materials Research

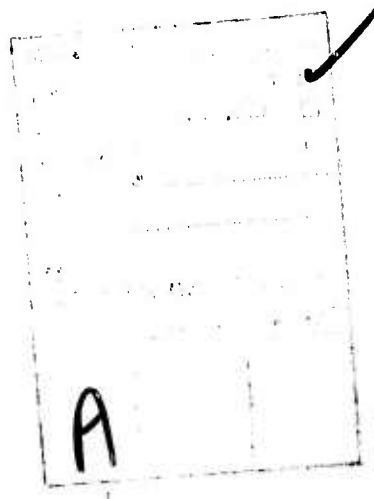
and

Marilyn J. Dodge

Optical Physics Division  
Institute for Basic Standards

ARPA Order No. . . . . 2620  
Program Code Number. . . . . 4D10  
Effective Date of Contract . . . . . January 1, 1974  
Contract Expiration Date . . . . . December 31, 1976  
Principal Investigator . . . . . Albert Feldman  
(301) 921-2840

The views and conclusions contained in this document are those of the authors and should not be interpreted as necessarily representing the official policies, either expressed or implied, of the Advanced Research Projects Agency or the U.S. Government.



## OPTICAL MATERIALS CHARACTERIZATION

### Abstract

The refractive index of a sample of hot-forged  $\text{CaF}_2$  was measured from 0.25  $\mu\text{m}$  to 8.0  $\mu\text{m}$  by means of the minimum-deviation method on a precision spectrometer. Data were obtained near 20°C and 34°C. Each data set was fitted to a three-term Sellmeier-type dispersion equation, which permits interpolation of refractive index as a function of wavelength within a few parts in  $10^5$ . With the index values obtained at the two temperatures, the change in index with temperature was calculated. The refractive index and values obtained for this specimen are compared with data previously published. Two new experimental arrangements have been constructed for the interferometric measurement of the thermal coefficient of refractive index, thermal expansion, and piezo-optic constants. The first permits measuring  $dn/dT$  and thermal expansion from -180 °C to +200 °C. The second is a highly stable and sensitive interferometer for measuring photoelastic constants in the visible, the near infrared, and the near ultraviolet. Thermal expansion data are obtained on CVD ZnSe,  $\text{CaF}_2$  and  $\text{BaF}_2$  between -100 °C and +120 °C and fitted to a third degree polynomial in temperature. We obtain  $dn/dT$  for CVD ZnSe at 632.8 nm over the same temperature range. The piezo-optic constants of fused silica and CVD ZnSe obtained with the new interferometer at 632.8 nm are in excellent agreement with values obtained by other methods.

## Table of Contents

1. Technical Report Summary. . . . .	1
1.1 Technical Problem. . . . .	1
1.2 General Methodology. . . . .	1
1.3 Technical Results. . . . .	1
1.4 Department of Defense Implications . . . . .	2
1.5 Implications for Further Research. . . . .	2
2. Technical Report. . . . .	3
2.1 Refractive Index and Its Temperature Coefficient for Hot-Forged Calcium Fluoride - Marilyn J. Dodge. . . . .	3
2.1.1 Introduction. . . . .	3
2.1.2 Experimental Technique. . . . .	3
2.1.3 Index Dts. . . . .	5
2.1.4 Temperature Coefficient of Index. . . . .	7
2.1.5 Conclusions . . . . .	7
2.1.6 Acknowledgments . . . . .	7
2.1.7 References. . . . .	7
2.2 Effect of Temperature and Stress on the Refractive Index of Window Materials - Albert Feldman, Deane Horowitz and Roy M. Waxler. . . . .	9
2.2.1 Introduction. . . . .	9
2.2.2 Apparatus and Experimental Method . . . . .	9
2.2.3 Results . . . . .	13
2.2.4 Acknowledgments . . . . .	13
2.2.5 References. . . . .	13

## OPTICAL MATERIALS CHARACTERIZATION

### 1. Technical Report Summary

#### 1.1 Technical Problem

Windows subjected to high-average-power laser radiation will undergo optical and mechanical distortion due to absorptive heating. If the distortion becomes sufficiently severe, the windows become unusable. Theoretical calculations of optical distortion in laser windows depend on the following material parameters; absorption coefficient, refractive index, change of index with temperature, thermal expansion coefficient, stress-optical constants, elastic compliances, specific heat, thermal conductivity and density. Our program has been established to measure refractive indices, changes of index with temperature, stress-optical constants, elastic compliances, and thermal expansion coefficients of candidate laser window materials.

#### 1.2 General Methodology

Laboratory experiments are conducted for measuring refractive indices, changes of index with temperature, stress-optical constants, elastic compliances, and thermal expansion coefficients.

The refractive indices of prismatic specimens are measured on precision spectrometers by using the method of minimum deviation. Two spectrometers are used. One instrument, which uses glass optics, is used for measuring refractive indices in the visible with an accuracy of several parts in  $10^6$ . The other instrument, which uses mirror optics, is used for measuring refractive indices in the ultraviolet and the infrared to an accuracy of several parts in  $10^5$ . Using both spectrometers we can measure refractive indices over the spectral region  $0.2 \mu\text{m}$  to  $50 \mu\text{m}$ .

We measure the coefficient of linear thermal expansion,  $\alpha$ , by a method of Fizeau interferometry. The interferometer consists of a specially prepared specimen which separates two flat plates. Interference fringes are observed due to reflections from the plate surfaces in contact with the specimen. We obtain  $\alpha$  by measuring the shift of these interference fringes as a function of temperature. We can measure  $\alpha$  from  $-180^\circ\text{C}$  to  $800^\circ\text{C}$ .

The change of refractive index with temperature,  $dn/dT$ , is measured by two methods. In the first method, we measure the refractive index with the precision spectrometers at two temperatures,  $20^\circ\text{C}$  and  $30^\circ\text{C}$ , by varying the temperature of the laboratory. This provides us with a measure of  $dn/dT$  at room temperature. The second method may be used for measuring  $dn/dT$  from  $-180^\circ\text{C}$  to  $800^\circ\text{C}$ . We obtain  $dn/dT$  from a knowledge of the expansion coefficient and by measuring the shift of Fizeau fringes in a heated specimen as a function of temperature. The Fizeau fringes are due to interferences between reflections from the front and back surfaces of the specimens.

We measure piezo-optic coefficients and elastic compliances using a combination of Twyman-Green and Fizeau interferometers. From the shift of fringes in specimens subjected to uniaxial or hydrostatic compression, we obtain the necessary data for determining all the stress-optical constants and elastic compliances.

In materials with small piezo-optic constants or in materials that cannot withstand large stresses, we use interferometers designed to measure fractional fringe shifts. At  $10.6 \mu\text{m}$  we use a modified Twyman-Green interferometer which has a sensitivity of  $0.01\lambda$ . At  $632.8 \text{ nm}$  we use a modified Dyson interferometer which has a sensitivity of  $0.002\lambda$ . When using these interferometers to measure piezo-optic constants we must know the elastic constants of the material under test.

#### 1.3 Technical Results

The refractive index of a sample of hot-forged  $\text{CaF}_2$  was measured from  $0.25 \mu\text{m}$  to  $8.0 \mu\text{m}$  by means of the minimum-deviation method on a precision spectrometer. Data were obtained near  $20^\circ\text{C}$  and  $34^\circ\text{C}$ . Each data set was fitted to a three-term Sellmeier-type dispersion equation, which permits interpolation of refractive index as a function of wavelength within a few parts in  $10^5$ . With the index values obtained at the two temperatures, the change in index with temperature,  $dn/dT$  was calculated. The refractive index and  $dn/dT$  values obtained for this specimen are compared with data previously published. (Section 2.1)

Two new experimental arrangements have been constructed for the interferometric measurement of the thermal coefficient of refractive index, thermal expansion, and piezo-optic constants. The first permits measuring  $dn/dT$  and thermal expansion from  $-180^\circ\text{C}$  to  $+200^\circ\text{C}$ . The second is a highly stable and sensitive interferometer for measuring photoelastic constants in the visible, the near infrared, and the near ultraviolet. Thermal expansion data are obtained on CVD  $\text{ZnSe}$ ,  $\text{CaF}_2$ , and  $\text{BaF}_2$  between  $-100^\circ\text{C}$  and  $+120^\circ\text{C}$  and fitted to a third degree polynomial in temperature. We obtain

dn/dT for CVD ZnSe at 632.8 nm over the same temperature range. The piezo-optic constants of fused silica and CVD ZnSe obtained with the new interferometer at 632.8 nm are in excellent agreement with values obtained by other methods. (Section 2.2)

#### 1.4 Department of Defense Implications

The Department of Defense is currently constructing high-power laser systems. Criteria are needed for determining the suitability of different materials for use as windows in these systems. The measurements we are performing provide data that laser system designers can use for determining the optical performance of candidate window materials.

#### 1.5 Implications for Further Research

Measurements of refractive index, change of index with temperature, thermal expansion, stress-optical constants and elastic compliances will be continued on candidate laser window materials. The wavelength of interest at present is 3.39  $\mu$ m which is within the wavelength range of interest to designers of chemical laser systems (3-5  $\mu$ m range).

Under consideration is the procurement of equipment to extend our interferometric measurements to 250 nm and 350 nm, wavelengths close to the lasing frequencies of the XeF and KrF lasers, respectively.

## 2. Technical Report

### 2.1 Refractive Index and Its Temperature Coefficient for Hot-Forged Calcium Fluoride

Marilyn J. Dodge

#### 2.1.1 Introduction

Optical distortion as a result of temperature gradients can occur in transparent or semi-transparent components of high-power laser systems at powers below that which would be required to melt or fracture the component [1-2]<sup>1</sup>. Knowledge of the refractive index,  $n$ , and temperature coefficient of refractive index,  $dn/dT$  of a candidate material to be used in a high-power laser system is necessary before the amount of optical distortion which might occur can be predicted. The study of these parameters is a part of an optical materials characterization program [3] which is currently in progress at NBS.

The increased use of high-power lasers in the 2-6  $\mu\text{m}$  wavelength region has resulted in a need for improved transparent component materials to be used in large, high-resolution optical systems. Ideally, the materials should be stronger, exhibit less scatter, and have lower absorption coefficients than the materials which are currently available [4]. Hot forging of alkali halides and alkaline-earth fluorides is one fabrication technique being developed to achieve these goals. Alkaline-earth fluorides are the materials of choice for use in the 2-6  $\mu\text{m}$  range [5]. If the new manufacturing technique does induce changes in the optical absorption of these materials, corresponding changes in the refractive index and  $dn/dT$  would also be expected from dispersion theory [6] and need to be determined.

John R. Fenter of the Air Force Materials Laboratory provided a large finished prism of hot-forged  $\text{CaF}_2$  manufactured by Harshaw Chemical Corp.<sup>2</sup> This specimen has a refracting angle near  $60^\circ$ , with one polished face about 4 cm x 5 cm and the other polished face about 4 cm x 6.5 cm. Unlike the synthetic single crystal  $\text{CaF}_2$  which is commercially available, the new material is polycrystalline.

#### 2.1.2 Experimental Technique

The index of refraction was determined by means of the minimum-deviation method using a precision spectrometer shown schematically in figure 1[7]. From the ultraviolet to 2.0  $\mu\text{m}$ , the index was determined at known emission wavelengths of mercury, cadmium, helium, and zinc. Beyond 2  $\mu\text{m}$ , a glow-bar was used for the radiant-energy source, and measurements were made at known absorption bands of water, carbon dioxide, polystyrene and 1,2-4 trichlorobenzene. A series of narrow-band interference filters was also used between 3.5  $\mu\text{m}$  and 6.5  $\mu\text{m}$ . A thermocouple with a cesium iodide window was used for the detector. The scale of this spectrometer can be read to 1.0 second of arc. The accuracy of this scale permits the determination of the refractive index of good optical quality material to within  $2 \times 10^{-5}$  over a wide wavelength range.

The index was determined from 0.2483 to 8.03  $\mu\text{m}$  and at average controlled room temperatures of  $20.8^\circ\text{C}$  and  $33.6^\circ\text{C}$ . Each set of experimental data was fitted to a three-term Sellmeier-type dispersion equation [8] of the form  $n^2 - 1 = \sum [A_j \lambda^2 / (\lambda^2 - \lambda_j^2)]$ . The index of refraction is represented by  $n$ ,  $\lambda$  is the wavelength of interest, the  $\lambda_j$ 's are the calculated wavelengths of maximum absorption and the  $A_j$ 's are the calculated oscillator strengths corresponding to the absorption bands. The  $\lambda_j$ 's and  $A_j$ 's are not intended to have any physical significance. Primary emphasis is given to procuring a mathematical fit of the measured data useful for interpolation.

---

1. Figures in brackets indicate the literature references at the end of a section.

2. The use of company and brand names in this paper are for identification purposes only and in no case does it imply recommendation or endorsement by the National Bureau of Standards, and it does not imply that the materials used in this study are necessarily the best available.



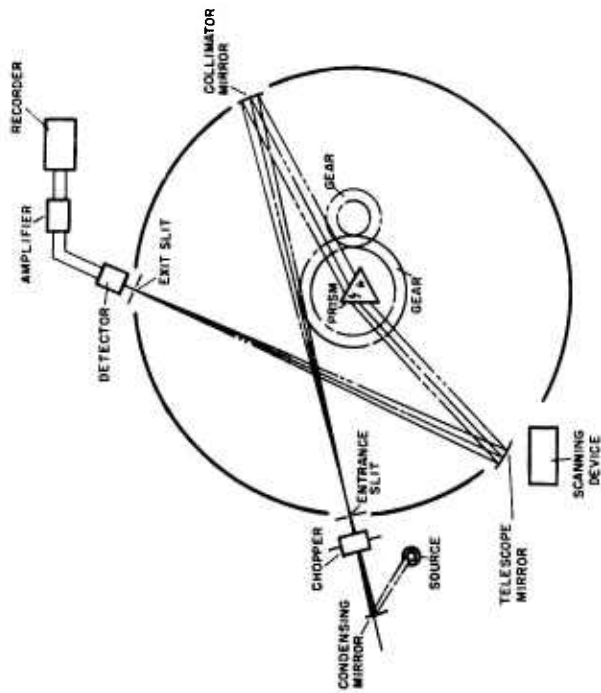


Fig. 1 Schematic diagram of the modified Gaertner precision spectrometer showing optical path. The prism is rotated at one-half the rotation rate of the telescope assembly by gear system, thus maintaining the condition of minimum-deviation for any wavelength. The scanning device drives the assembly which scans the spectrum to identify lines or bands and determine their approximate scale positions.

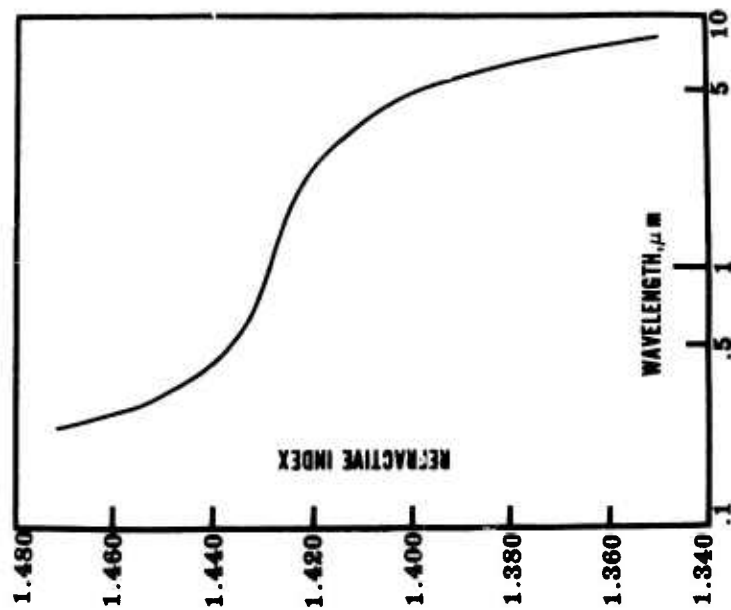


Fig. 2 Refractive index of hot-forged  $\text{CaF}_2$  as a function of wavelength (logarithmic scale). Data at  $20.8^\circ\text{C}$  were calculated from the dispersion equation of the form  $n^2 - 1 = \sum A_j \lambda_j^2 / (\lambda^2 - \lambda_j^2)$ .

### 2.1.3 Index Data

The constants calculated for each dispersion equation, the number of wavelengths fitted and the average absolute residual (the average difference between the experimental values and the calculated values) are given in table 1.

Table 1: Constants for Dispersion Equations

Constant	20.8°C	33.6°C
$A_1$	0.98584551	0.97066991
$A_2$	0.05290246	0.06792205
$A_3$	4.2816899	4.1634415
$\lambda_1$	0.07218116	0.07115659
$\lambda_2$	0.14114719	0.13670627
$\lambda_3$	36.465937	35.984292
No. of Wavelengths	69	47
Average Absolute residual of index $\times 10^5$	1.9	1.9

It should be emphasized that these constants refer specifically to this sample of hot-forged  $\text{CaF}_2$ , at the stated temperatures, and should be used for interpolation only within the wavelength range of the experimental data, or approximately 0.25 to 8.0  $\mu\text{m}$ . The average absolute residual is an indication of the overall accuracy of the experimental data. Generally, the largest residuals were in the IR beyond 5  $\mu\text{m}$ , where 35 strong atmospheric absorption bands existed between 5.0 and 7.3  $\mu\text{m}$ . Because of the large size of the prism and the apparent excellent quality of the material, these bands were sharp and their minima were easily determined. Therefore, the index determinations are not considered to be any less accurate than in the UV or near IR. The wavelengths of these atmospheric bands were assigned from values in the literature [9,10]. The uncertainties in the wavelength values would be difficult to define due to differences in the laboratory conditions and the existence of many weak bands which could affect the wavelengths of nearby strong bands. An error of 0.1% in wavelength would result in an index residual of  $9 \times 10^{-5}$  in this particular sample.

The refractive index was calculated at regular wavelength intervals for each temperature with the appropriate fitted parameters. The results of the 20.8°C data are plotted as a function of wavelength in figure 2.

The index values obtained for this specimen are compared in figure 3 with those obtained by I. H. Malitson on single crystal  $\text{CaF}_2$  [10]. The single crystal data is represented by the "zero" line. The differences reach a minimum between 0.7 and 0.9  $\mu\text{m}$  where the hot-forged  $\text{CaF}_2$  is only  $-0.5 \times 10^{-5}$  less than the single crystal. A maximum difference of  $-6.6 \times 10^{-5}$  between the two types of  $\text{CaF}_2$  exists at 0.28  $\mu\text{m}$  and 4.8  $\mu\text{m}$ . The index variance at 0.28  $\mu\text{m}$  is probably the result of a weak absorption band near 0.3  $\mu\text{m}$ . The Harshaw catalog [11] shows transmission runs for two grades of  $\text{CaF}_2$ , the UV grade in which this band does not appear, and the optical grade, sold for use in IR components, in which the band does exist. Assuming this band did not exist in the single crystal studied previously, the differences in index would become more negative, reaching the maximum  $\Delta n$ , then receding as the index of the new  $\text{CaF}_2$  approaches that of the single crystal in the red region of the spectrum.

The maximum magnitude of  $\Delta n$  at 4.8  $\mu\text{m}$  is not as easily explained. The absorption bands and interference filter used for index measurements between 4 and 5  $\mu\text{m}$  generally yield low residuals in highly transmitting materials such as  $\text{CaF}_2$  when fitted to the dispersion equation. The Sellmeier equation will fail completely in an area of strong absorption in the material, but will attempt to fit data through a region of weak absorption yielding larger residuals in the area of the band. In this study, the residuals between 4 and 5  $\mu\text{m}$  were an order of magnitude higher than the ones immediately on either side of the region where they agreed well with the overall average of  $1.9 \times 10^{-5}$ . The Sellmeier fit called for higher wavelengths in this region, indicating that the experimental

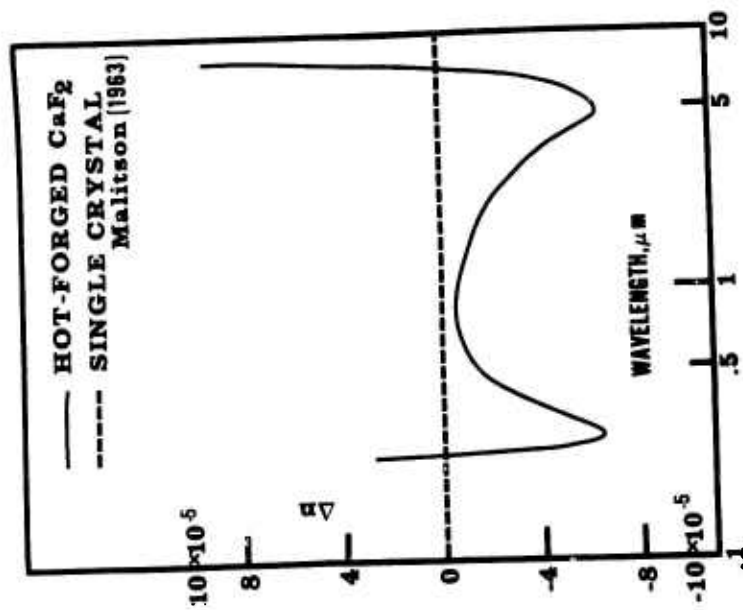


Fig. 3 The differences in index of hot-forged  $\text{CaF}_2$  from single crystal  $\text{CaF}_2$  at  $20.8^\circ\text{C}$  as a function of wavelength (logarithmic scale). The index of the single crystal is represented by the zero line.

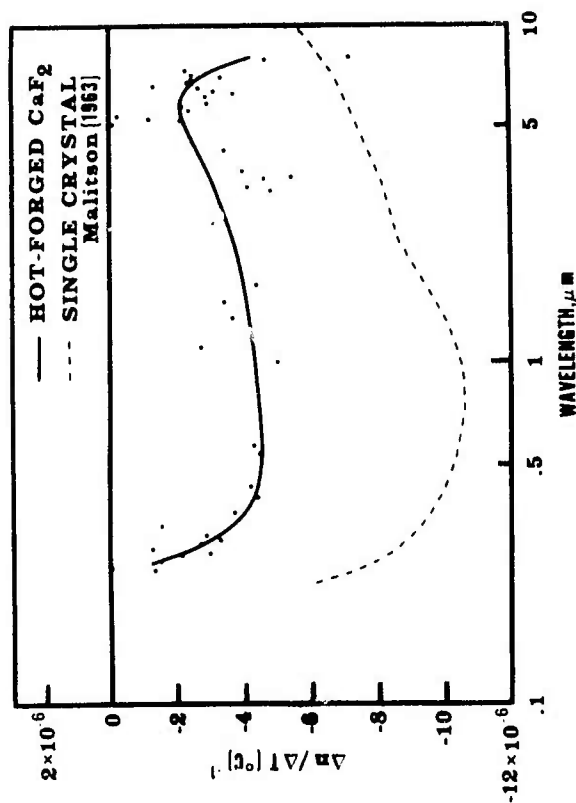


Fig. 4 Temperature coefficient of index as a function of wavelength (logarithmic scale) of  $\text{CaF}_2$ . The solid line represents  $\Delta n/\Delta T(^{\circ}\text{C})^{-1}$  calculated from the fitted values at  $20.8^\circ\text{C}$  and  $33.6^\circ\text{C}$  for the hot-forged  $\text{CaF}_2$  and the data points (x's) represent  $\Delta n/\Delta T$  values calculated from the measured index values. The dashed line shows  $\Delta n/\Delta T$  for single crystal  $\text{CaF}_2$  from the literature.

index values were lower than what would be expected in a region of normal dispersion. From dispersion theory, this could be an indication of a weak absorption band near 5  $\mu\text{m}$ . There are indications of a weak absorption band in the 3-4  $\mu\text{m}$  region of ionic crystals including fluorides [3]. Most absorption studies that have been made on the polycrystalline material have been done at the specific laser wavelengths of HF (2.7  $\mu\text{m}$ ), DF (3.8  $\mu\text{m}$ ) and CO (5.25  $\mu\text{m}$ ). To get a clear picture of the absorption characteristics in this area it would be necessary to run an absorption curve as a function of wavelength.

#### 2.1.4 Temperature Coefficient of Index

The index values calculated with the fitted parameters at the two temperatures were used to determine  $\Delta n/\Delta T(^{\circ}\text{C})^{-1}$  as a function of wavelength and are indicated in figure 4 by the solid line. Also shown in this figure for comparison purposes, is the  $\Delta n/\Delta T$  curve for the single crystal material referenced previously. Generally the hot-forged  $\text{CaF}_2$  shows much smaller  $\Delta n/\Delta T$  values than the single crystal. The maximum  $\Delta n/\Delta T(^{\circ}\text{C})^{-1}$  of the new material over the wavelength range studied is  $-4.5 \times 10^{-6}$  between 0.5 and 0.6  $\mu\text{m}$ , or a little less than half the  $\Delta n/\Delta T(^{\circ}\text{C})^{-1}$  reported for the single crystal in the same region. The ratio is about the same at 2  $\mu\text{m}$  where  $\Delta n/\Delta T(^{\circ}\text{C})^{-1}$  of the hot-forged sample is  $-3.9 \times 10^{-6}$ , but at 6  $\mu\text{m}$   $\Delta n/\Delta T$  of the polycrystalline material is only about a third of that given for the single crystal material, or  $-2.2 \times 10^{-6}$ . Beyond 6  $\mu\text{m}$ ,  $\Delta n/\Delta T(^{\circ}\text{C})^{-1}$  increases to  $-4.3 \times 10^{-6}$  at 8.0  $\mu\text{m}$ . The negative  $\Delta n/\Delta T$  suggests that the thermal expansion dominates the change in refractive index with temperature. Moreover  $\Delta n/\Delta T$  is expected to increase as either the ultraviolet or infrared limits of transmittance are approached [14]. The deviations from this expected behavior could be another indication of some type of absorption in the 5  $\mu\text{m}$  region. The  $\Delta n/\Delta T(^{\circ}\text{C})^{-1}$  values that were calculated from the measured data are shown as data points in figure 4. The magnitude of the values between 3 and 4  $\mu\text{m}$  increase to almost  $1.5 \times 10^{-6}$  higher than those calculated from the smoothed data, but then decrease to about  $2 \times 10^{-6}$  less than the smoothed values at about 4.5  $\mu\text{m}$ , giving an anomalous appearance. The smoothed  $\Delta n/\Delta T$  values are considered accurate within  $1 \times 10^{-6}$ . Other investigators have stated that when determining  $\Delta n/\Delta T$  by the technique used in this study fourth decimal place accuracy in index is required to achieve a 10 percent accuracy in  $\Delta n/\Delta T$  [15].

#### 2.1.5 Conclusions

This is the first detailed study of the refractive properties of hot-forged  $\text{CaF}_2$ . From the standpoint of the reduced temperature coefficient of refractive index, it appears that components fabricated from this material could produce less optical distortion than those made from synthetic single crystal  $\text{CaF}_2$ . However, since the hot-forged manufacturing technique is still in a stage of development and improvement, and in light of the refractive index anomaly which appeared in the 4 to 5  $\mu\text{m}$  region of primary interest to laser systems designers, further studies on other samples of this material should be considered. It should not be assumed that the refractive properties of this sample are necessarily typical of what can be expected of future production runs of hot-forged  $\text{CaF}_2$ .

#### 2.1.6 Acknowledgments

The author expresses sincere appreciation to Warren K. Gladden for his technical assistance in this study.

#### 2.1.7 References

- |   |  |
|---|--|
| [1] Sparks, M., J. Appl. Phys. <u>42</u> , 5029 (1971).   | [5] I.B.I.D.   |
| [2] Loomis, J. S. and Bernal, E. G., "Laser Induced Damage in Optical Materials: 1975," p. 126, NBS Special Publication 435, US Govt. Printing Office, Wash. (1976).                                      | [6] Jenkins, F. A. and White, H. E., <u>Fundamentals of Optics</u> , 3rd ed. McGraw-Hill Book Company, Inc., (1957).   |
| [3] Feldman, A., Malitson, I., Horowitz, D., Waxler, R. M. and Dodge, M., "Laser Induced Damage in Optical Materials: 1974," NBS Special Publication 414, p. 141, US Govt. Printing Office, Wash. (1974). | [7] Rodney, William S. and Spindler, Robert J., J. Res. Nat'l. Bur. Stds. (US), <u>51</u> , 123, (1953).               |
| [4] Newberg, R. T., Readey, D. W., Newborn, H. A., and Miles, P. A., Proceedings, Fourth Annual Conference on Infrared Laser Window Materials, p. 445, AFML (Jan. 1975).                                  | [8] Sutton, Loyd E. and Stavroudis, Orestes N., J. Opt. Soc. Am. <u>51</u> , 901 (1961).                               |
|   | [9] Downie, A. R., Magoon, M. C., Purcell, Thomasine and Crawford, Bryce Jr., J. Opt. Soc. Am. <u>43</u> , 941 (1953). |

- [10] Benedict, W. S., Claassen, H. H. and Shaw, J. H., J. Res. NBS 49, 91 (1952).
- [11] Malitson, I. H., Applied Optics 2, 110 (1963).
- [12] Harshaw Optical Crystals, The Harshaw Chemical Co., 22, (1967).
- [13] Hass, Marvin, Proceedings, Fifth Annual Conference on Infrared Laser Window Materials p. 850, UDRI (Feb., 1976).
- [14] Krishnan, R. S., Progress in Crystal Physics, Vol. 1, Ch V, p. 146 (Vijayanathan, S. at the Central Art Press; Chetput, Madras 31, 1958).
- [15] Ibid.

## 2.2 Effect of Temperature and Stress on the Refractive Index of Window Materials

Albert Feldman, Deane Horowitz and Roy M. Waxler

### 2.2.1 Introduction

When high-power radiation propagates through a laser window the residual absorption causes a temperature rise in the window. The temperature distribution in the window is, in general, non-uniform and hence will distort the wavefront of the beam. This distortion arises from three sources: the direct change of the refractive index due to a change in temperature; the change of optic path due to a change of thickness with temperature; and the change of refractive index due to stresses induced by thermal gradients. If the distortion is sufficiently severe, the laser window becomes unusable [1]. In order to predict the distortion of a laser beam wavefront from the laser energy deposited in a window, one requires certain material parameters. These parameters include absorption coefficient, refractive index,  $n$ , change of refractive index with temperature,  $dn/dT$ , the piezo-optic constants,  $q_{ij}$ , thermal expansion coefficients,  $\alpha$ , and elastic constants,  $S_{ij}$  or  $c_{ij}$  [1]. It is the purpose of the Optical Materials Characterization Program at the National Bureau of Standards to measure  $n$ ,  $dn/dT$ ,  $q_{ij}$ ,  $\alpha$ , and if necessary  $S_{ij}$  [2].

In this paper we describe two new apparatuses constructed under this program. The first apparatus consists of a cryogenically cooled furnace that permits us to measure  $\alpha$  and  $dn/dT$  interferometrically from  $-180^\circ\text{C}$  to  $+200^\circ\text{C}$ . The second apparatus consists of a polarizing interferometer that is capable of measuring fringe shifts to within a precision of  $\lambda/500$  at  $632.8\text{ nm}$ . This precision is useful for measuring the piezo-optic constants of materials at low stresses. The use of the interferometer is limited in the ultraviolet by the cutoff of calcite which is at about  $300\text{ nm}$ , and in the infrared by the useful range of the Soleil-Babinet compensator which is at about  $1.15\text{ }\mu\text{m}$ . The Soleil-Babinet compensator is used for measuring fringe shifts.

We present data obtained with the two new instruments. We have measured the photoelastic constants of chemical vapor deposited (CVD) ZnSe and fused silica and found excellent agreement with previously reported values [3,4,5]. We have measured the linear expansion coefficient of CVD ZnSe,  $\text{CaF}_2$ , and  $\text{BaF}_2$  from  $-100^\circ\text{C}$  to  $+120^\circ\text{C}$  and the data were fitted to a third degree power expansion in temperature. The fit for  $\text{CaF}_2$  and  $\text{BaF}_2$  agrees with available published data to within about 1% [6]. There was a slightly poorer agreement of our fit for CVD ZnSe to single crystal values of ZnSe [7], however, the observed difference is not necessarily significant because of the different materials measured. We have also measured  $dn/dT$  of CVD ZnSe at  $632.8\text{ nm}$  and have found a value 2% smaller than our previously reported value [8]. We attribute this difference to our improved measurement technique; however, our value differs significantly from Mukai et al. [9].

For brevity we do not discuss the phenomenological theory of photoelasticity, because this theory has been described adequately in the literature [10].

### 2.2.2 Apparatus and Experimental Method

The thermal expansion coefficient and  $dn/dT$  are measured by the method of Fizeau interferometry. The general method for making these measurements has been described in the literature [11].

To measure thermal expansion we measure as a function of temperature the shift of Fizeau fringes between two optical flats separated by the specimen. To measure  $dn/dT$  we measure as a function of temperature the shift of Fizeau fringes formed from reflections from the front and back surfaces of a specimen polished plane parallel. We have constructed a compact apparatus for obtaining  $\alpha$  and  $dn/dT$  from  $-180^\circ\text{C}$  to  $+200^\circ\text{C}$ . A schematic of the apparatus is shown in figure 1.

The furnace is constructed from a cylinder of copper 37 mm in diameter by 75 mm high with walls 6 mm thick to permit rapid transfer of heat. A commercial band heater, which is clamped around the furnace, generates 175 W with an input of 120 VAC.

The furnace rests at the bottom of an evacuable chamber 100 mm in diameter by 150 mm tall. Protruding from the bottom is a copper rod, 12 mm in diameter by 150 mm long, that conducts heat away from the furnace to the liquid nitrogen reservoir. Thus, we can stabilize the temperature in the furnace at an arbitrary point by balancing the heat input from the heater with the heat leak to the liquid nitrogen.

The specimen rests within the furnace over a depression that is milled at an angle of  $1^\circ$  with respect to the furnace axis in order to deflect laser beam reflections to the side. Holes are drilled at several locations within the furnace to allow placement of thermocouples in contact with the specimen and to allow the pressure within the furnace to equalize with the pressure outside the furnace. Two thermocouples measure the temperature at the top and at the bottom of the specimen. A copper cover with a window allows access of laser radiation to the specimen in the furnace while maintaining a uniform thermal environment around the specimen. All windows in the system are tilted at a  $1^\circ$  angle to eliminate unwanted reflections.

We find that the system operates well when filled with a helium exchange gas of several millimeters pressure. The helium environment has several advantages over air or vacuum. During cooldown, products in the air condense on the system optics and hence interfere with the laser beam. With vacuum, the thermal response of the system is sluggish because of poor heat transfer between the furnace, the heat leak, and the specimen. In addition, there is a large temperature difference between the two thermocouples. With the helium present, the maximum temperature differential measured with the two thermocouples across a 12 mm thick specimen is less than 1 K at a given temperature.

The procedure used for measuring  $dn/dT$  or  $\alpha$  consists of first cooling the specimen to approximately liquid nitrogen temperature. Sufficient time is allowed for the two thermocouple readings to agree to within 1 K. The furnace is then heated very slowly until a fringe minimum is observed on a strip chart recorder monitoring the Fizeau fringe intensity. The temperature is then recorded. Subsequently, the furnace is heated rapidly and after a convenient number of fringes has been observed, power to the furnace is cut back to allow the thermocouple readings to equilibrate while the temperature is slowly rising. At a fringe minimum, the temperature is recorded. The heating process is repeated until the maximum desired temperature is achieved.

The fringe counts and their corresponding temperatures are punched onto computer tape and the fringe count,  $\Delta N$  is then obtained as a power series expansion of the temperature by computer. For thermal expansion measurements, we obtain an expression for the relative incremental thickness change of the specimen

$$\frac{\Delta t}{t_0} = A_1 T + A_2 T^2 + A_3 T^3 \quad (1)$$

where  $t_0$  is the specimen length at room temperature,  $\Delta t$  is the incremental length, and  $A_1, A_2, A_3$  are the expansion parameters. The derivative of eq. (1) with respect to  $T$  gives  $\alpha$ .

We obtain  $dn/dT$  by calculating first the incremental change of refractive index  $\Delta n$  as a function of temperature with the formula

$$\Delta n = \frac{\Delta N \lambda}{2t_0} - n_0 \frac{\Delta t}{t_0} \quad 1 + \frac{\Delta t}{t_0}^{-1} \quad (2)$$

where  $n_0$  is the room temperature refractive index and  $\Delta N$  and  $\Delta t/t_0$  are representations of power series in temperature. The slope of the curve gives  $dn/dT$ , which we tabulate at a variety of temperatures.

The polarizing interferometer we have constructed for measuring piezo-optical constants is shown in figure 6. This interferometer is based on a design by Dyson [12], which was further modified by Green [13] for measuring thermal expansion and  $dn/dT$ . Our design, which is a slight modification of Green's, is capable of measuring fringe shifts to within a precision of  $\lambda/500$  at 632.8 nm. The modification involves a change of position of the quarter wave plate within the interferometer.

The output of a helium-neon laser is propagated through a Glan-Thompson polarizer and is focused into a Wollaston prism. The prism splits the beam into two orthogonally polarized beams. The intensities of the two beams are balanced by a rotation of the polarizer. The beams are then collimated and made parallel to each other by passing through a second lens. The outer beam is intercepted by the specimen. Both beams are now brought to a focus at a rear mirror after propagating through a quarter wave plate. The two beams then return through the system; the central beam retraces its path while the outer beam propagates along the opposite side of the interferometer. Double passage through the quarter wave plate interchanges the states of polarization of the two beams. Thus, when the two beams are rejoined at the Wollaston prism, they exit as a combined beam at an angle with respect to the incident beam. A spatial filter and beam expander are placed in the exit beam to eliminate spurious laser radiation. A Soleil-Babinet compensator and a second Glan-Thompson prism are then used to analyze the state of polarization of the exit beam. The output fringe patterns are observed with a silicon matrix vidicon camera and a television monitor.

This interferometer has several advantages over conventional Twyman-Green interferometers: It is highly stable with respect to motion of system elements because both beams traverse the same optics, hence the optic path changes in both arms tend to be equal. In addition, the close proximity of the arms minimizes the effect of thermal currents, which are further reduced by placement of a cover over the interferometer part of the apparatus. Moreover, the fringe shifts are analyzed with ellipsometric techniques which have great inherent precision.

At the position of the specimen shown in figure 5, the radiation is polarized in the horizontal plane, hence, the fringe shift per unit applied uniaxial stress,  $\Delta N/\Delta P$ , for an isotropic material will depend on the piezo-optic constant  $q_{12}$ . If we shift the specimen to the outer return beam, where the radiation is vertically polarized, the fringe shift will depend on  $q_{11}$ . The expression for the piezo-optic constant is

$$q = \frac{2}{n} \frac{\lambda}{t_0} \frac{\Delta N}{\Delta P} + (n-1) S_{12} \quad (3)$$

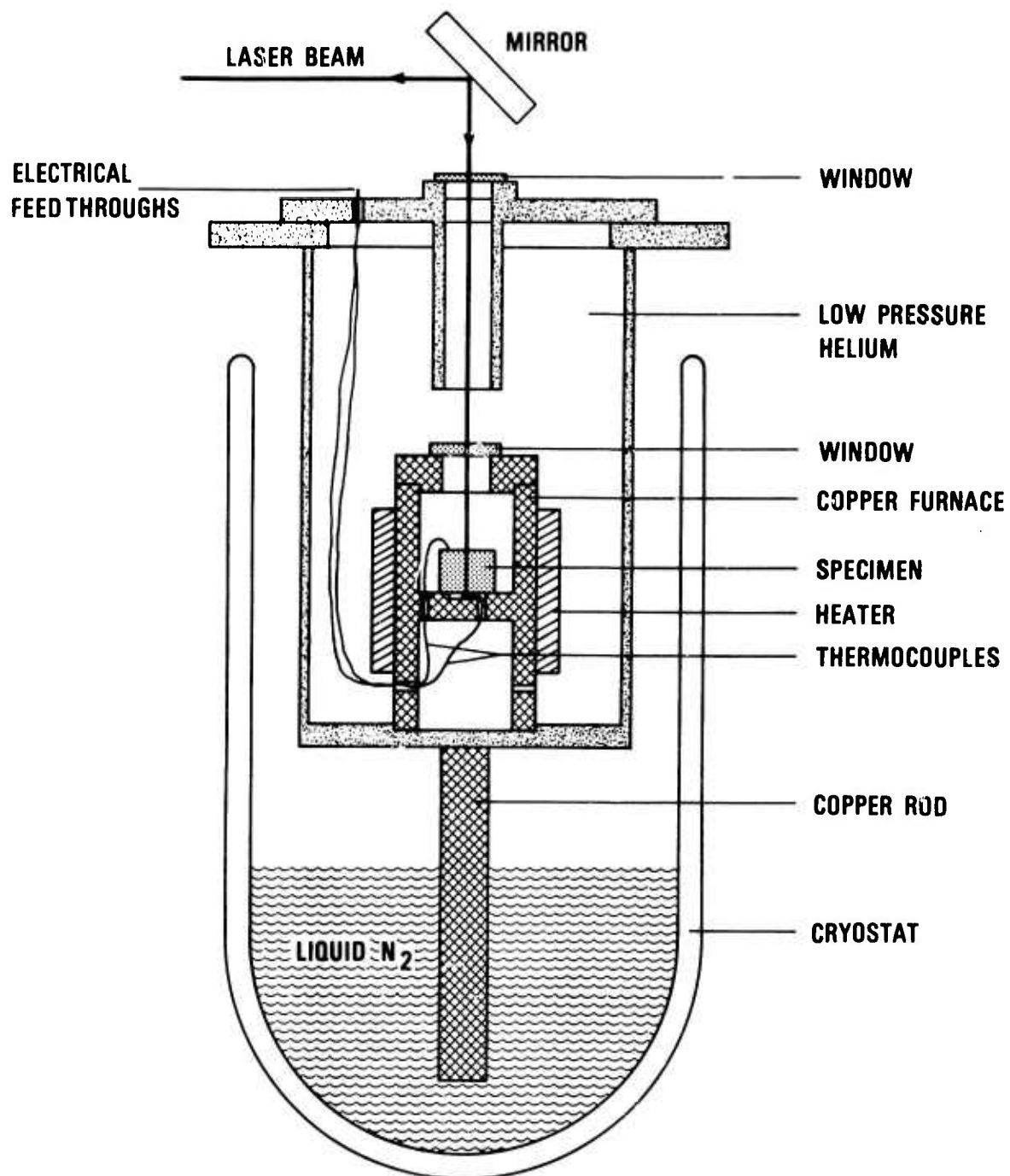


Fig. 5 Cryogenically cooled furnace for measuring thermal expansion and change of refractive index with temperature. The specimen shown is for  $dn/dT$ .



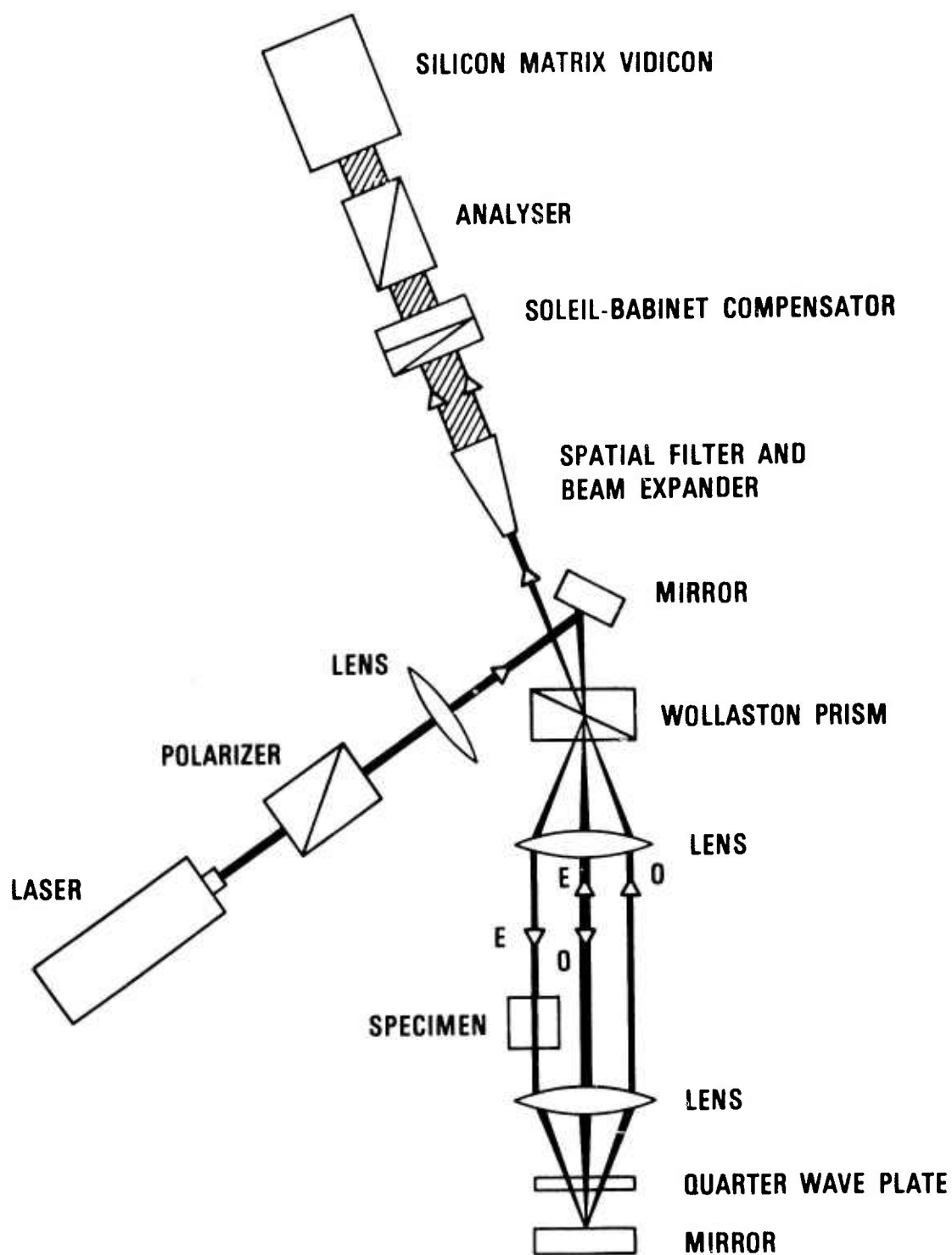


Fig. 6 Modified Dyson interferometer for measuring piezo-optic constants.

where  $q = q_{11}$  for vertical polarization,  $q = q_{12}$  for horizontal polarization,  $\lambda$  is the wavelength of the radiation and  $S_{12}$  is the elastic compliance component. In this equation  $t_0$  lacks a factor of two present in the equation for the Twyman-Green interferometer because the modified Dyson interferometer is used only as a single pass instrument.

Sample preparation and the method of applying stress have been described in the literature and so will not be discussed here [14]. The direction of stress is always vertical.

### 2.2.3 Results

In table 2, we list the thermal expansion parameters (eq. 1) of CVD ZnSe that we have obtained with seven runs on three specimens. The bottom row gives a statistically weighted average of the coefficients and the errors are the standard deviation of the mean. These values permit us to calculate the linear thermal expansion coefficient between  $-100^\circ\text{C}$  and  $+120^\circ\text{C}$ . These coefficients differ from our earlier reported values [8], however, we believe our present values are better because of our improved experimental technique. The thermal expansion coefficients calculated with these parameters are slightly higher than values obtained by Novikova [7], however, the type of material we have used differs from that used by Novikova. Moreover, Zhdanova and Sergeev report that the thermal expansion coefficient of ZnSe varies with free carrier and impurity content [15].

In table 3, we list the thermal expansion parameters we have obtained for  $\text{CaF}_2$  and  $\text{BaF}_2$  between  $-100^\circ\text{C}$  and  $+120^\circ\text{C}$ . When these parameters are used to calculate  $\alpha$ , we find agreement within about 1% with values published in the literature [6].

The expressions we have obtained for the thermal expansion facilitate our measurement of  $dn/dT$  by the interferometric method. In table 4, we list the values of  $dn/dT$  we have obtained for CVD ZnSe at 632.8 nm from  $-100^\circ\text{C}$  to  $+120^\circ\text{C}$ . The value we obtain at  $25^\circ\text{C}$  is  $1.06 \times 10^{-4} \text{ K}^{-1}$  which is 2% smaller than our previously reported values. We attribute this difference to an improvement of our measurement technique; however, we cannot explain the discrepancy of our value with that of Mukai et al. [9].

The piezo-optic constants of fused silica and CVD ZnSe have been measured at 632.8 nm with the modified Dyson interferometer. The results obtained for fused silica, given in table 5, agree extremely well with those of Primak and Post [5]. The standard deviation we give in the table represents the deviation from a linear least squares fit of optic path change as a function of stress. The actual accuracy is not as good because of possible systematic errors in the system, but these we believe to be less than 2%. Such systematic errors would include stress gradients.

The results we have obtained for CVD ZnSe are given in table 6. The agreement obtained with our previously reported values [3] is remarkably good, where the errors in the table are attributed mainly to the uncertainty in  $S_{12}$ . The data also agree, within experimental error, with the results of Goldstein et al. [4].

### 2.2.4 Acknowledgment

We thank the Raytheon Company for the CVD ZnSe.

### 2.2.5 References

- [1] Sparks, M., J. Appl. Phys. 42, 5029 (1971); Jasperse, J. R., and Gianino, P. D., J. Appl. Phys. 43, 1686 (1972); Bendow, B., and Gianino, P. D., Applied Physics 2, 1 (1973); Bendow, B., Gianino, P. D., Hordvik, A., and Skolnik, L. H., Optics Comm. 7, 219 (1973).
- [2] Feldman, A., Malitson, I., Horowitz, D., Waxler, R. M., and Dodge, M., in *Laser Induced Damage in Optical Materials*, edited by A. J. Glass and A. H. Guenther, National Bureau of Standards Special Publication 414 (1974) pp. 141.
- [3] Feldman, A., Waxler, R. M., and Horowitz, D., in *Optical Properties of Highly Transparent Solids*, edited by S. S. Mitra and B. Bendow (Plenum Publishing Corp., N.Y., 1975) pp. 517.
- [4] Goldstein, L. F., Thompson, J. S., Schroeder, J. B., and Slattey, J. E., Applied Optics 14, 2432 (1975).
- [5] Primak, W., and Post, D. J., J. Appl. Phys. 30, 779 (1959).
- [6] Baily, A. C., and Yates, B., Proc. Phys. Soc. 91, 390 (1967); Sharma, S. S., Proc. Indian Acad. Sci. A31, 261 (1950).
- [7] Novikova, S. I., Soviet Physics-Solid State 3, 129 (1961) [Fizika Tverdogo Tela 3, 178 (1961)].
- [8] Feldman, A., Malitson, I. H., Horowitz, D., Waxler, R. M., and Dodge, M., in *Proceedings of the 4th Annual Conference on Infrared Laser Window Materials*, (1974) pp. 117.

- [9] Mukai, H., Krok, P., Kepple, G., Harris, R., and Johnston, G., in *Proceedings of the Fifth Conference on Infrared Laser Window Materials* (1975) pp. 225.
- [10] Nye, J. F., in *Physical Properties of Crystals* (Oxford University Press, London, 1957) pp. 243-254.
- [11] Waxler, R. M., Cleek, G. W., Malitson, I. H., Dodge, M. J., and Hahn, T. A., *J. Res. Nat. Bur. Stand. (U.S.)* 75A, 163 (1971).
- [12] Dyson, J., *Interferometry as a Measuring Tool* (The Machinery Publishing Co., Ltd., Brighton, 1970).
- [13] Green, F., in *Optical Instruments and Techniques, 1969*, edited by J. H. Dickson (Oriel Press Limited, New Castle upon Tyne, England, 1970) pp. 189-198.
- [14] Feldman, A., and McKean, W. J., *Rev. Sci. Instrum.* 46, 1588 (1975).
- [15] Zhdanova, V. V., and Sergeev, V. P., *Soviet Physics-Solid State* 14, 1859 (1973) [*Fizika Tverdogo Tela* 14, 2153 (1972)].

Table 2. Tabulation of expansion parameters of CVD ZnSe for  
-100 °C < T < +120 °C

$$\Delta t/t_0 = A_1 T + A_2 T^2 + A_3 T^3$$

Run #	Specimen #	$A_1 (10^{-6} \text{ K}^{-1})$	$A_2 (10^{-9} \text{ K}^{-2})$	$A_3 (10^{-11} \text{ K}^{-3})$
1	1	7.75 ± 0.08	5.24 ± 0.31	-1.40 ± 0.30
2	1	7.35 ± 0.03	4.62 ± 0.16	-1.67 ± 0.15
3	1	7.33 ± 0.05	4.80 ± 0.17	-1.47 ± 0.22
4	1	7.23 ± 0.04	5.19 ± 0.17	-1.26 ± 0.17
5	2	7.24 ± 0.05	5.51 ± 0.25	-1.53 ± 0.22
6	3	7.28 ± 0.04	5.94 ± 0.13	-1.44 ± 0.13
7	3	7.30 ± 0.04	5.27 ± 0.15	-1.34 ± 0.16
Weighted Average		7.29 ± 0.02	5.26 ± 0.17	-1.45 ± 0.07

Errors are the standard deviation of the mean.

Table 3. Expansion parameters of CaF<sub>2</sub> and BaF<sub>2</sub> for

$$\Delta t/t = A_1 T + A_2 T^2 + A_3 T^3$$

	$A_1 (10^{-6} \text{ K}^{-1})$	$A_2 (10^{-9} \text{ K}^{-2})$	$A_3 (10^{-11} \text{ K}^{-3})$
CaF <sub>2</sub>	18.4 ± 0.1	16.4 ± 0.3	-3.7 ± 0.3
BaF <sub>2</sub>	18.1 ± 0.1	11.5 ± 0.3	-2.0 ± 0.3

Table 4.  $dn/dT$  of CVD ZnSe at 632.8 nm

Temperature	$dn/dT$ ( $10^{-5} \text{ K}^{-1}$ )
-100	9.3
- 80	9.6
- 60	9.8
- 40	10.0
- 20	10.2
0	10.4
20	10.6
40	10.7
60	10.9
80	11.0
100	11.1
120	11.2

Table 5. Piezo-optic constants of fused silica at 632.8 nm

	Present Work	Primak and Post <sup>a</sup>
$q_{11}$	$0.42 \pm 0.002^b$	0.44
$q_{12}$	$2.70 \pm 0.006^b$	2.71

Units -  $10^{-12} \text{ m}^2/\text{N}$ <sup>a</sup>Reference [5]<sup>b</sup>Errors represent the standard deviation of the experimental data to a straight line least squares fit. Accuracy is believed to be within 2%.

Table 6. Piezo-optic constants of CVD ZnSe at 632.8 nm

	Present Work	Previous Work	
$q_{11}$	$0.17 \pm 0.04$	$0.17 \pm 0.05^a$	$0.22 \pm 0.05^b$
$q_{12}$	$-1.44 \pm 0.04$	$-1.44 \pm 0.04^a$	$-1.48 \pm 0.05^b$

Units -  $10^{-12} \text{ m}^2/\text{N}$ <sup>a</sup>Reference [3]<sup>b</sup>Reference [4]

U.S. DEPT. OF COMM. BIBLIOGRAPHIC DATA SHEET	1. PUBLICATION OR REPORT NO. NBSIR 76-1115	2. Gov't Accession No.	3. Recipient's Accession No.
4. TITLE AND SUBTITLE  Optical Materials Characterization		5. Publication Date August 1976	
		6. Performing Organization Code	
7. AUTHOR(S) A. Feldman, D. Horowitz, R. Waxler, and M. Dodge		8. Performing Organ. Report No.	
9. PERFORMING ORGANIZATION NAME AND ADDRESS  NATIONAL BUREAU OF STANDARDS DEPARTMENT OF COMMERCE WASHINGTON, D.C. 20234		10. Project/Task/Work Unit No. 3130442	
		11. Contract/Grant No.	
12. Sponsoring Organization Name and Complete Address (Street, City, State, ZIP) Advanced Research Projects Agency Arlington, Virginia 22209		13. Type of Report & Period Covered Interim 2/1/76 - 7/31/76	
		Sponsoring Agency Code	
15. SUPPLEMENTARY NOTES 100101			
16. ABSTRACT (A 200-word or less factual summary of most significant information. If document includes a significant bibliography or literature survey, mention it here.) <p>The refractive index of a sample of hot-forged <math>\text{CaF}_2</math> was measured from 0.25 <math>\mu\text{m}</math> to 8.0 <math>\mu\text{m}</math> by means of the minimum-deviation method on a precision spectrometer. Data were obtained near 20°C and 34°C. Each data set was fitted to a three-term Sellmeier-type dispersion equation, which permits interpolation of refractive index as a function of wavelength within a few parts in <math>10^5</math>. With the index values obtained at the two temperatures, the change in index with temperature was calculated. The refractive index and values obtained for this specimen are compared with data previously published. Two new experimental arrangements have been constructed for the interferometric measurement of the thermal coefficient of refractive index, thermal expansion, and piezo-optic constants. The first permits measuring <math>dn/dT</math> and thermal expansion from -180 °C to +200 °C. The second is a highly stable and sensitive interferometer for measuring photoelastic constants in the visible, the near infrared, and the near ultraviolet. Thermal expansion data are obtained on CVD ZnSe, <math>\text{CaF}_2</math> and <math>\text{BaF}_2</math> between -100 °C and +120 °C and fitted to a third degree polynomial in temperature. We obtain <math>dn/dT</math> for CVD ZnSe at 632.8 nm over the same temperature range. The piezo-optic constants of fused silica and CVD ZnSe obtained with the new interferometer at 632.8 nm are in excellent agreement with values obtained by other methods.</p>			
17. KEY WORDS (six to twelve entries; alphabetical order; capitalize only the first letter of the first key word unless a proper name; separated by semicolons) $\text{BaF}_2$ ; $\text{CaF}_2$ ; fused silica; interferometry; photoelasticity; piezo-optic constants; refractive index; thermal coefficient of refractive index; thermal expansion coefficient; ZnSe.			
18. AVAILABILITY <input checked="" type="checkbox"/> Unlimited <input type="checkbox"/> For Official Distribution. Do Not Release to NTIS <input type="checkbox"/> Order From Sup. of Doc., U.S. Government Printing Office Washington, D.C. 20402, SD Cat. No. C13 <input checked="" type="checkbox"/> Order From National Technical Information Service (NTIS) Springfield, Virginia 22151		19. SECURITY CLASS (THIS REPORT)  UNCLASSIFIED	21. NO. OF PAGES  20
		20. SECURITY CLASS (THIS PAGE)  UNCLASSIFIED	22. Price  \$3.50